

PRELIMINARY TESTING OF NANOPARTICLE EFFECTIVENESS IN BINDER JETTING APPLICATIONS

Alta C. Bailey*, Abbey Merriman*, Amelia Elliott*, and Mufeed M. Basti†

*Manufacturing Demonstration Facility, Oak Ridge National Lab, Oak Ridge, TN 37932

† Department of Chemistry, North Carolina A&T State University, Greensboro, NC
27401

Abstract

Binder jetting works by selectively depositing a binder with an inkjet print head into layers of powdered material. Compared with other metal Additive Manufacturing (AM) processes, binder jetting has significant potential for near-term adoption in manufacturing environments due to its reliability and throughput. The Achilles heel of binder jetting, however, is the inability to produce fully dense, single-alloy materials. The lack of density in printed binder jet parts is strictly dictated by the packing factor of the powder feedstock. Adding nanoparticles during printing will not only increase the part's packing factor but may also serve as a sintering aid. This study focuses on the effect of both the binder and nanoparticles on the final part density. As an unintended consequence of high nanoparticle loading, printed parts underwent a significant increase in porosity during the curing process. This unintended consequence is the apparent result of the nanoparticles blocking the exit of the solvent vapor during the curing step. Additionally, nanoparticle use for densification is validated with SEM imagery.

Introduction

Additive Manufacturing (AM), *aka* 3D printing, is a step-wise technology used to create 3-dimensional structures slice by slice. AM technology encompasses Material Jetting, Binder Jetting, Material Extrusion, Powder Bed Fusion, Vat Photopolymerization, Directed Energy Deposition, and Sheet Lamination [1]. Binder jetting is unique among AM processes due to its room-temperature processing and ability to shape any powdered material with the use of a binder. The drawback of binder jetting, however, is the challenge in achieving full density of the shaped powder feedstocks. One strategy for improving the density of binder jet prints is to incorporate nanoparticles in the inkjet fluid, which fill the voids between the powder particles. The challenge with jetting nanoparticles, however, is their effect on viscosity of the jetted binder, which makes inkjet deposition difficult or impossible [2]. Before approaching ink-jetting of metal nanoparticles for the densification of metal systems, the effect of the nanoparticle and binder mixture on the overall density of a powder system should be investigated. The purpose is to determine the effectiveness of nanoparticles in a binder jet binder system on the final density of a stainless steel powder system.

This manuscript has been authored by UT-Battelle, LLC under Contract No. DE-AC05-00OR22725 with the U.S. Department of Energy. The United States Government retains and the publisher, by accepting the article for publication, acknowledges that the United States Government retains a non-exclusive, paid-up, irrevocable, worldwide license to publish or reproduce the published form of this manuscript, or allow others to do so, for United States Government purposes. The Department of Energy will provide public access to these results of federally sponsored research in accordance with the DOE Public Access Plan (<http://energy.gov/downloads/doe-public-access-plan>).

Background

The Binder Jetting process works by selectively distributing a binder into layers of powdered material via inkjet. A thin layer of powder is spread over the print area, and binder is selectively dispersed out of a print head into the shape of a layer of the 3D part. The process is then repeated, layer by layer, until the object is complete (Figure 1). After printing, the binder is cured, the part is removed from the powder bed, and the part is infiltrated with a secondary, lower melting point material via capillary infiltration while being sintered. The primary metal material system produced by binder jetting is a printed stainless steel infused with bronze. Although this material system has its merits [3], fully dense, single-alloy with Binder Jetting is desired.

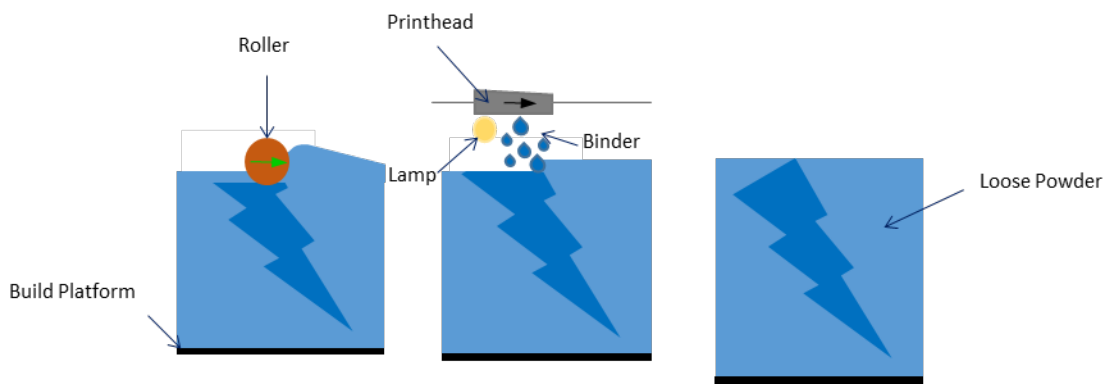


Figure 1: Spreading of the Powder, Binder Deposition and curing lamp, Completed Part Encased in Loose Powder

Because Binder Jetting uses a powder bed, the packing factor of the powder material feedstock dictates the final printed part density. The packing factor is the fractional volume in a structure that is occupied by particles. The higher the packing factor, the higher the density of the printed part and less shrinkage the part experiences during post-processing. The packing factor for a powder system can be increased by filling the void spaces left between larger particles with smaller particles. Bai. *et al.* proved that having a bimodal distribution of powder while maintaining the median particle size can improve the packing factor of the powder bed and sintered density [4]. In 1961 McGeary, found that to produce efficient packing in dry powder systems, the difference between particle diameters should be at least sevenfold [5] Generally, when the size ratio of course particles to fine particles, decreases, the packing density is lowered [6].

Previous attempts were made at exploring the effect of nanoparticles on part density by deposition of nanoparticle suspensions on top of pre-sintered, low-density, stainless steel pucks shaped via binder jetting [7]. Stainless steel nanoparticles were suspended in solutions with varying properties, such as polarity and pH, and deposited on top of the printed steel puck skeletons. Results showed that the printed pucks acted as a filtering media, and solution fluid passed through while the nanoparticles piled on the top of the puck samples. An increase in density in the samples was noticed for certain solution properties; however, the location of the nanoparticles within the sample was undetectable after sintering. This was due to the

nanoparticles themselves agglomerating into larger particles during sintering, and as they were the same material as the printed skeleton, no color difference was offered as a clue to nanoparticle location. In this study, copper nanoparticles were chosen to be deposited into stainless steel powder because of the color difference between the two metals. Also, instead of manipulating dispersion components of the binder (ethylene glycol and/or diethylene glycol), the binder itself was used in this study as a baseline for testing the effects of nanoparticles on final part density. By suspending copper nanoparticles in binder then adding the mixture to the stainless steel, we produce a nanoparticle, binder, and powder system that is more analogous to the Binder Jetting process.

Methods

Stainless steel powder (ExOne® S4-30, 30 μm, spherical), nano-Copper (US Nano, 99.9% purity, 100nm, spherical, bulk density: 0.21 g/cm³), and binder (ExOne® Lab Binder 04) were mixed in varying volume ratios and cast into bar geometries. Three groups of test specimens were prepared. The first group, the control, and the second group, the secondary control, were comprised of only stainless steel powder and binder. In Group 1, four test bars, having dimensions of 10mm x 10mm x 60mm were printed on the X1-Lab™ machine. The second group, Group 2, of test bars were shaped via a Teflon™ mold into similar geometries. Mixtures, at a ratio of 14 g of stainless steel to 1 mL of binder, were hand mixed and incrementally transferred into a mold. Each sample was cured at 200°C for 2 hours. The curing was done at typical settings to remove solvent in the binder and allow the polymer to crosslink and hold the powder together.

For Group 3, a parent solution of copper nanoparticles and binder was made by mixing 100 g of nano-Copper with 70 mL of binder. This mixture was then hand mixed for 10-15 min to ensure uniformity. Targeting percent of void space left between the larger stainless steel particles, varying amounts of the parent solution of nanoparticles was added to a controlled amount of stainless steel powder, according to Table 1, and mixed by hand for approximately 5 minutes. The mass of nanoparticle parent solution was calculated based on the parent solution's packing factor, τ , and the targeted fraction of void space between stainless steel particles. The mass of nanoparticle solution chosen was based on filling the void space in the stainless steel powder feedstock at 4, 7, 10, 20, 40, and 70 percent. In other words, the stainless steel particles were mixed with an amount of copper nanoparticles in solution that would fill 4, 7, 10, 20, 40, and 70 percent of the void space present in the stainless steel powder system. The amount of parent solution needed to target the aforementioned void space was calculated according to Equations 1 & 2:

$$\tau = \frac{\left(\frac{mass_{\beta}}{\rho_{true,\beta}}\right)}{\left[(Binder\ Volume) + \left(\frac{mass_{\beta}}{\rho_{true,\beta}}\right)\right]} \quad (1)$$

$$mass_{\gamma} = \left(\frac{(1 - PF_{\alpha})(Skeletal\ Volume)(Target\ Void\ Space)}{\tau}\right) \times \rho_{\gamma} \quad (2)$$

α = Primary Material

β = Secondary Material

γ = Parent Solution: Binder & Secondary Material
 τ = Calculated Packing Factor of Binder-Secondary Mixture
 PF_{α} = Packing Factor of Primary Material
 ρ_i = Density
 $\rho_{true,i}$ = True Density

A mixture consistency was targeted that allowed for casting of the bars without either separation of the paste during deposition or weeping of excess binder. For the mixtures that were too dry, additional binder was added in 1 mL quantities. For mixtures that were too saturated, they were allowed to set out overnight, then heated to 200°C, allowing time for the solvent in the binder to evaporate. For both situations, binder was added and/or dried until the right consistency was reached. Each of the six mixtures was then transferred to Teflon™ molds and molded into 2 bars each with approximate dimensions of 10mm x 10 mm x 60 mm. The molded bars were then transferred to an oven and cured at 200°C for 2 hours to allow the polymer to hold the powders together. After curing, the bars were sintered under a 4% hydrogen 96% argon cover gas per the sintering schedule in Figure 2. Samples were then cut using a non-ferrous blade, mounted in a clear epoxy, and polished down to a glass finish for imaging. Images were taken with a 16MP camera and a Hitachi SU3400 Scanning Electron Microscope.

Table 1: nCu/STS Sample Preparation Quantities

Specimen	% Targeted of Void Space	Stainless Steel Powder	Parent Solution Added
1	4 %	42 g	2.03 g
2	7 %	42 g	3.56 g
3	10 %	42 g	5.09 g
4	20 %	42 g	10.17 g
5	40 %	42 g	20.35 g
6	70 %	42 g	35.61 g

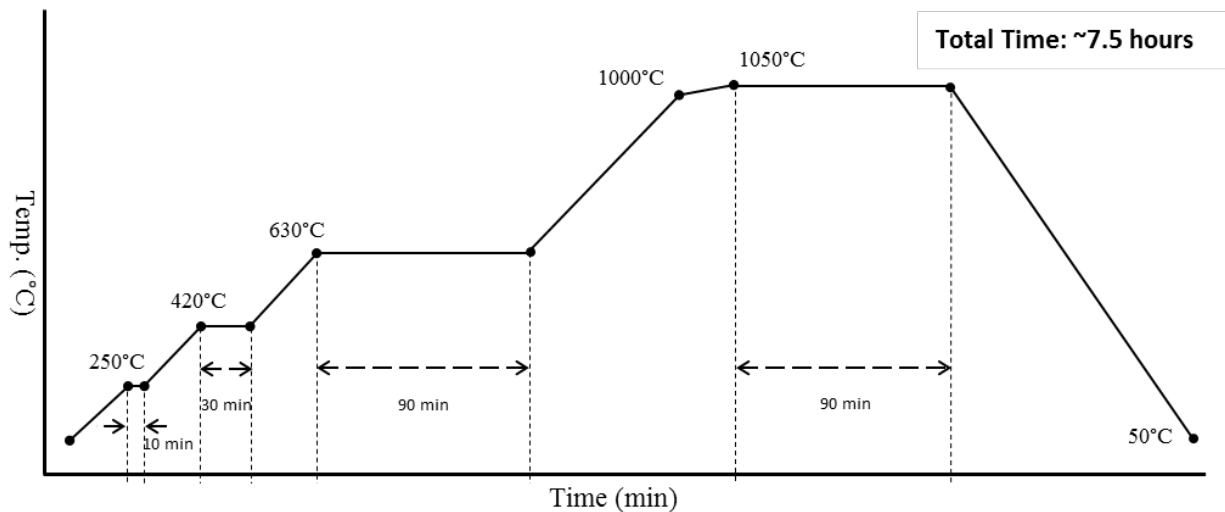


Figure 2: Sintering Schedule

Results & Discussion

Effects of Nanoparticles on Curing

During curing, significant foaming occurred in samples with higher concentrations of nanoparticles, a phenomenon that had not been observed in any previous experimentation. Comparing the samples reveals that as the amount of nano-copper increases, the visible porosity of the sample increases, with the sample with the highest loading of nanoparticles having the highest visible porosity. Images of these samples after sintering, cutting, mounting, and polishing are provided in Figure 3.

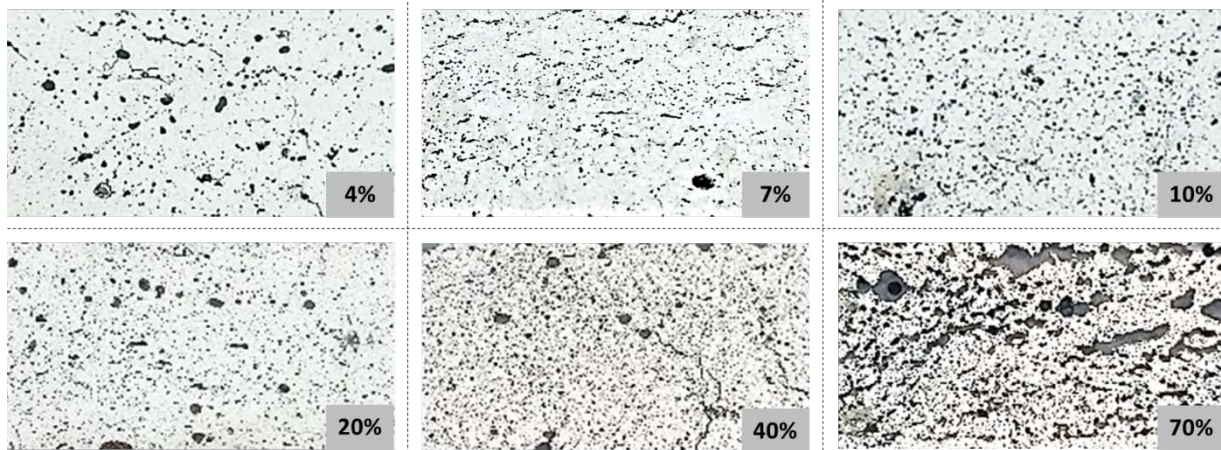


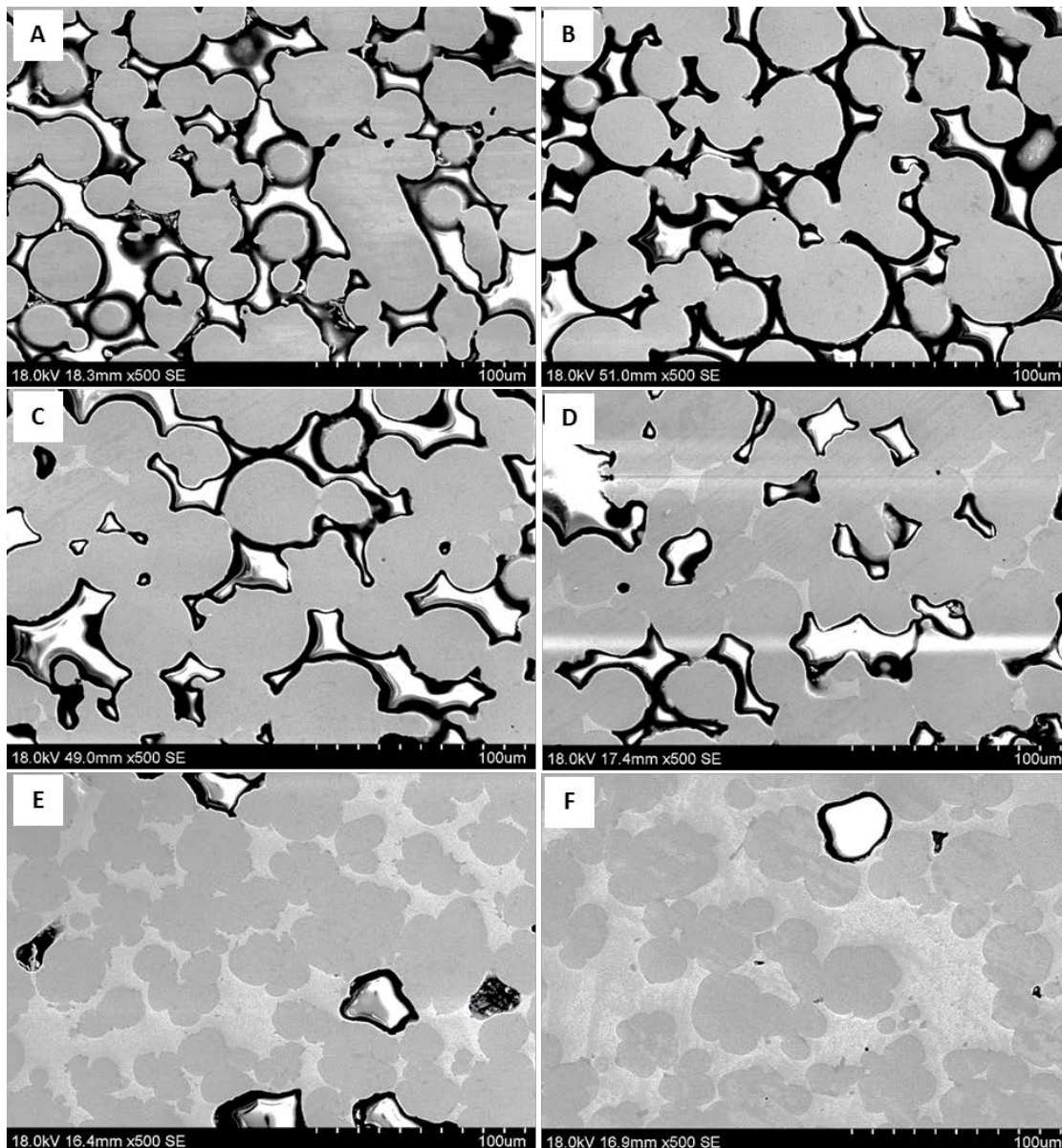
Figure 3: Micrographs of Sintered and Mounted Samples

Two factors must be considered to explain the foaming phenomena observed in the cured samples. The first factor is the potentially high loading of binder solution due to the high surface area of the nanoparticles. During curing, the solvent in the binder solution is driven off over the course of an hour. With an increase in binder, the off-gassing of the solvent during curing potentially occur more rapidly, forcing the opening of large pores and cavities. This is unlikely however since samples highly saturated with ExOne binder have been cured under similar conditions previously, and no foaming had been observed. Therefore, the likely cause of foaming in the samples is the blockage by the nanoparticles of flow paths for the solvent vapor to escape. In other words, the nanoparticles potentially fulfilled their role by filling the void space between the larger powder particles, however in doing so they have prevented the solvent in the binder from escaping during the curing cycle, creating large cavities in the samples. Future work will include controlling the binder loading and examination of the cast samples prior to curing under SEM to observe potential factors in the creation of the cavities.

Effects of Nanoparticles on Sintering

After curing, the samples were sintered, cut into cross-sections, and polished for imaging of regions that were representative of the overall porosity of the sample were chosen. The SEM images in Figure 4 show a cross section of each sample. In each image, the stainless steel particles are shown as large, interconnected circles of the same color. As the copper content increases, it becomes more visible between the larger stainless steel particles, represented by a lighter shade. We see that as the amount of nano-copper increases in the void space, sintering of

the stainless steel increases due to the copper behaving as a sintering aid. The high thermal conductivity of copper makes it great for use in applications that require the movement of heat into and out of a system (heat exchangers, bottom of cookware, etc.). Because of copper's high thermal conductivity, it is able to facilitate the movement of a large amount of heat very quickly, unlike stainless steel. As the temperature in the furnace increases, the copper nanoparticles undergo inter-particle coalescence due to surface melting influenced by their small size [8]. Afterwards, the particles, which have now coalesced, resemble that of bulk copper and are able to move large amounts of heat to the stainless steel, influencing the sintering behavior of stainless steel. This phenomena readily presents itself at higher amounts of nano-copper as can be seen in images E) and F) in Figure 4, where we observe sintering of the stainless steel encapsulated by the molten copper.



Even though the nano-copper acts as a sintering aid, more significant to this study is the behavior of nanoparticles in a bimodal system for use in binder jetting applications. Understanding that nanoparticles cause foaming at higher concentrations during the curing process, is of great importance to the overall goal of densification. Solving this is key before introducing nanoparticles, in quantities high enough to fill the void space, into the binder jetting process. Such solution would allow for parts with complex alloy compositions that are useful in applications such as energy storage, tooling, and catalysis.

Conclusions & Future Work

Binder jet-printed materials must undergo significant shrinkage to reach full density due to the low packing factor of the powder feedstocks. Adding nanoparticles to the powder feedstocks could potentially increase this packing factor and reduce the amount of shrinkage needed. Previous efforts to quantify the effects of stainless steel nanoparticles on stainless steel powder packing density resulted in the inability to distinguish the location of the nanoparticles within the sintered object, as the nanoparticles and powder were made of the same material. Copper nanoparticles were added to a Binder jet binder system and mixed with stainless steel powder feedstock for the purpose of showing contrast between the nanoparticles and powder particles. The expectation for this mixture was that, after sintering, the nanoparticles will fill the voids between the stainless steel powder particles and overall improve material density while avoiding shrinkage. The unexpected outcome of this work was discovered during the curing phase, where the solvent is driven off of the binder system and escapes through the gaps between the particles. During this curing step, the mixtures with higher concentrations of nanoparticles experienced significant foaming or expansion of macro-sized voids within the part topology. It is hypothesized that this foaming is due to the nanoparticles themselves improving the packing factor of the powder system to the point that the solvent in the binder system is unable to escape, creating large cracks and voids. Future work to explore this phenomenon will include the following:

- 1) Varying the size of the nanoparticles and exploring its effect on off-gassing due to the change in surface area available to the solvent in the binder for wetting.
- 2) Determining the optimum void fill fraction to nanoparticle to binder ratio to significantly increase the density of the printed part while reducing the off-gassing effects of the solvent in the binder.

Acknowledgements

The authors would like to thank Dr. Parans Paranthaman for the use of his nanoparticle hood and assistance in handling the nanoparticles. We would also like to thank Dr. Peeyush Nandwana for his help in imaging the samples presented in this work.

References

- [1] ASTM International, Standard Terminology for Additive Manufacturing - General Principles - Terminology, West Conshohocken, Pennsylvania, 2015.
- [2] B. Derby and N. Reis, "Inkjet Printing of Highly Loaded Particulate Suspensions," *MRS Bulletin*, vol. 28, no. 11, pp. 815-818, November 2003.
- [3] ExOne, "Ulterra," [Online]. Available: http://www.exone.com/Portals/0/ResourceCenter/CaseStudies/X1_CaseStudies_All%209.pdf. [Accessed 2016].
- [4] Y. Bai, G. Wagner and C. B. Williams, "Effect of Bimodal Powder Mixture on Powder Packing Density and Sintered Density in Binder Jetting of Metals," in *2015 Annual International Solid Freeform Fabrication Symposium*, Austin, TX, 2015.
- [5] R. K. McGeary, "Mechanical Packing of Spherical Particles," *Journal of the American Ceramic Society*, vol. 44, no. 10, pp. 513-522, 1961.
- [6] J. Zheng, W. B. Carlson and J. S. Reed, "The Packing Density of Binary Powder Mixtures," *Journal of the European Ceramic Society*, vol. 15, pp. 479-483, 1995.
- [7] A. Elliott, S. AlSalihi, A. L. Merriman and M. M. Basti, "Infiltration of Nanoparticles into Porous Binder Jet Printed," *American Journal of Engineering and Applied Sciences*, vol. 9, no. 1, pp. 128-133, 2016.
- [8] D. Mott, J. Galkowski, L. Wang, J. Luo and C.-J. Zhong, "Synthesis of Size-Controlled and Shaped Copper Nanoparticles," *Langmuir*, vol. 23, no. 10, pp. 5740-5745, 2007.
- [9] E. M. Sachs, J. S. Haggerty, M. J. Cima and P. A. Williams, "THREE-DIMENSIONAL PRINTING TECHNIQUES". United States of America Patent 5,204,055, 20 April 1993.
- [10] W. G. Kreyling, M. Semmler-Behnke and Q. Chaudhry, "A complementary definition of nanomaterial," *Nano Today*, vol. 5, no. 3, pp. 165-168, June 2010.
- [11] R. A. Yetter, R. A. Grant and S. F. Son, "Metal particle combustion and nanotechnology," *The Combustion Institute*, vol. 32, no. 2, pp. 1819-1838, 2009.
- [12] J. C. Sung, B. L. Pulliam and D. A. Edwards, "Nanoparticles for drug delivery," *TRENDS in Biotechnology*, vol. 25, no. 12, p. 563, 2007.
- [13] J. S. Kim, E. Kuk, K. N. Yu, J.-H. Kim, S. J. Park, H. J. Lee, S. H. Kim, Y. K. Park, Y. H. Park, C.-Y. Hwang, Y.-K. Kim, Y.-S. Lee, D. H. Jeong and C. Myung-Haing, "Antimicrobial effects of silver nanoparticles," *Nanomedicine: Nanotechnology, Biology, and Medicine*, vol. 3, pp. 95-101, 2007.
- [14] L. M. Katz, K. Dewan and R. L. Bronaugh, "Nanotechnology in cosmetics," *Food and Chemical Toxicology*, vol. 85, pp. 127-137, 2015.
- [15] L. Mu and R. L. Sprando, "Application of Nanotechnology in Cosmetics," *Pharmaceutical Research*, vol. 27, no. 8, pp. 1746-1749, 2010.
- [16] L. Rashidi and K. Khosravi-Darani, "The Applications of Nanotechnology in Food Industry," *Critical Reviews in Food Science and Nutrition*, vol. 51, no. 8, p. 723, 2011.
- [17] J.-Y. Qiu, Y. Hotta and K. Watari, "Enhancement of Densification and Thermal Conductivity in AlN Ceramics by Addition of Nano-Sized Particles," *Journal of American Ceramic Society*, vol. 89, pp. 377-380, 2006.

- [18] O. S. Ivanova, C. B. Williams and T. A. Campbell, "Additive Manufacturing (AM) and Nanotechnology: Promises and Challenges," *Rapid Prototyping Journal*, vol. 19, no. 5, pp. 353-364, 2013.
- [19] J. G. Bai, T. G. Lei, J. N. Calata and G.-Q. Lu, "Control of nanosilver sintering attained through organic binder burnout," *Journal of Materials Research*, vol. 22, no. 12, pp. 3494-3500, 2007.
- [20] M. Wang and P. Kwon, "Improving Densification of Zirconium Tungstate with Nano Tungsten Trioxide and Sintering Aids," in *Proceedings of the ASME 2013 International Manufacturing Science and Engineering Conference*, Madison, WI, 2013.

ACKNOWLEDGMENT OF FUNDING

This material is based upon work supported by the U.S. Department of Energy, Office of Science, Office of Advanced Manufacturing, under contract number DE-AC05-00OR22725.